

Cosmic Rays in the Interstellar Medium

Serena Viti, Estelle Bayet, Thomas W. Hartquist, Thomas A. Bell,
David A. Williams, and Manda Banerji

Abstract In this article we will highlight the importance of cosmic rays for the chemistry of the interstellar medium (ISM) in our own Milky Way as well as in external galaxies. We will review the methodologies employed to determine the cosmic ray ionization rates in the ISM, how cosmic rays rates can influence the determination of the mass of a galaxy and, finally, how cosmic rays affect star formation and its rate.

S. Viti (✉) · D.A. Williams

Department of Physics and Astronomy, University College London, Gower St., London, WC1E 6BT, UK

e-mail: sv@star.ucl.ac.uk; daw@star.ucl.ac.uk

E. Bayet

Sub-Department of Astrophysics, University of Oxford, Denys Wilkinson Building, Keble Road, Oxford, OX1 3RH, UK

e-mail: Estelle.Bayet@astro.ox.ac.uk

T.W. Hartquist

School of Physics and Astronomy, University of Leeds, Leeds, LS2 9JT, UK

e-mail: tw@ast.leeds.ac.uk

T.A. Bell

Centro de Astrobiología, CSIC-INTA, 28850, Madrid, Spain

e-mail: tab@cab.inta-csic.es

M. Banerji

Institute of Astronomy, University of Cambridge, Madingley Road, Cambridge, CB3 0HA, UK

Department of Physics and Astronomy, University College London, Gower St., London, WC1E 6BT, UK

e-mail: mbanerji@ast.cam.ac.uk

1 The Chemistry of Cosmic Rays

Cosmic rays are superthermal particles, which are mostly ionized hydrogen and helium. In the interstellar medium (ISM) they initiate and drive most of the interstellar chemistry by colliding with and ionising atoms and molecules. During ionization they transfer energy to the ejected electrons and by doing so they heat the gas. Moreover, secondary photons generated by cosmic rays are a source of photodissociation and ionization in a UV shielded gas. Hence cosmic rays also help to maintain the ionization fraction deep within molecular clouds.

While the energies of cosmic rays range from MeV to ultrarelativistic values, the rays that most ionize the ISM are those with energies ≤ 1 GeV. Unfortunately below ~ 2 GeV the observed flux from Earth has to be corrected by the effects of the solar wind and such corrections, and hence the cosmic ray ionization rate, can be rather uncertain [33]. We will describe later different ways one can determine such rate but first it is worth summarizing the general chemical effects of cosmic rays on the molecular and atomic content of the ISM.

Low energy cosmic rays are capable of ionizing all atoms and molecules, including the most abundant ones. In Table 1 we list the important reactions involving cosmic rays for the most abundant elements.

In particular, it is the creation of the H^+ , He^+ and H_2^+ ions that then drive much of the chemistry in the ISM. This is because many ion-molecule reactions, unlike neutral-neutral exchanges, are rapid and occur at almost every collision, even at low temperatures (~ 10 K), typical of cold molecular clouds. For example, with molecular hydrogen being the most abundant molecule in dark clouds, the ion H_2^+ will always encounter an H_2 molecule and form a new species, H_3^+ which in turn will react with oxygen or carbon monoxide. On the other hand, the ion He^+ is very destructive in that it easily dissociates molecules via charge transfer.

In summary, cosmic rays are key in initiating oxygen and carbon chemistries and ultimately more complex chemistry. The rate of ionization induced by cosmic rays is therefore a parameter of fundamental importance.

1.1 Determining the Cosmic Ray Ionization Rate in the ISM

The most direct way to determine the cosmic ray ionization rate within our own Galaxy is from direct measurements on Earth. However, as mentioned in the previous section, below ~ 2 GeV the observed flux must be corrected for the effects of the solar wind but the uncertainties from these corrections can be as high as a factor of 3 at 1 GeV and much higher for energies less than 0.3 GeV [13]. There are alternative ways to measure this rate, in our own as well as in external galaxies, essentially from studies of the products of ion-neutral chemistry inside the molecular clouds. Different species have been used in recent years but generally one can assume that every cosmic ray ionization of H_2 will eventually produce a molecule of H_3^+ and so the abundance of this ion is often used as a tracer of the

Table 1 Chemical reactions involving cosmic rays

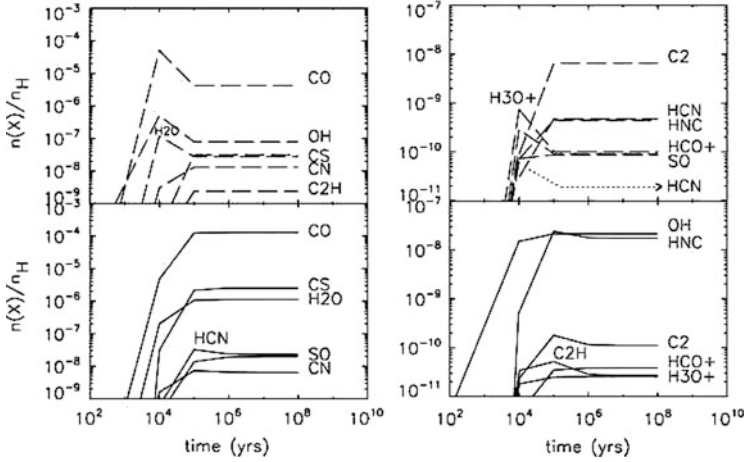
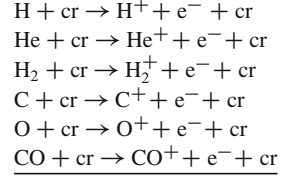


Fig. 1 Taken from Bayet et al. ([5], Fig. 4): the influence of cosmic ray ionization rate variations on selected molecular abundances are plotted for a model where $\zeta = 100\zeta_o$ (top panels) and a model where $\zeta = \zeta_o$ (bottom panels)

cosmic ray ionization rate, referred also as ζ . This however is only possible in a steady-state scenario where one can ‘fit’ the required cosmic ray ionization rate to the observed (or derived from OH observations) abundance of H_3^+ in steady state [11, 16], essentially by treating ζ as a free parameter. The inferred values of ζ are of the order of 10^{-17} s^{-1} , which is now routinely called the ‘standard’ ISM cosmic ray ionization rate, or ζ_o . However, more recent observational studies of H_3^+ towards several lines of sight in the Galactic Plane have in fact derived higher values for ζ , of the order of 10^{-16} s^{-1} , averaged over all the lines of sight [18].

A step further has been taken by e.g. Meijerink et al. [23] and Bayet et al. [7] where the authors look at the variations of the whole chemistry as the cosmic ray ionization rate is varied. Figure 1 shows an example taken from Bayet et al. [7]: here ζ is varied from the $5 \times 10^{-17} \text{ s}^{-1}$ to two orders of magnitude above this value and some molecular species, such as OCS, SO_2 and H_2CS stand out as being the most sensitive species to variation in the cosmic ray ionization rate. In principle, therefore, assuming all other physical properties are known, one could derive ζ in a sample of molecular clouds by observing these species.

2 The Chemistry in Cosmic Ray Dominated Regions

The fact that we can now identify molecular species sensitive to variations in cosmic rays leads to the possibility of using astrochemistry as a tool for the characterization of regions where the cosmic ray ionization rate is higher than in our own galaxy. For example, the high spatial density of massive star formation in mergers and starburst galaxies (e.g. [1, 2, 30]) creates regions of extremely high cosmic ray energy density, up to about 10,000 times that in the Milky Way Galaxy. Papadopoulos [26] has proposed that these large energy densities alter the heating rates and ionization fractions in dense gas ($n(\text{H}_2) \geq 10^4 \text{ cm}^{-3}$) in the UV-shielded cores that contain much of the molecular gas in these galaxies, so that these cosmic ray dominated regions (CRDRs) have different initial conditions for star formation. These conditions affect the subsequent evolution of the gas and may even lead to a top-heavy initial mass function and bimodal star formation [26, 27].

2.1 Theoretical Considerations

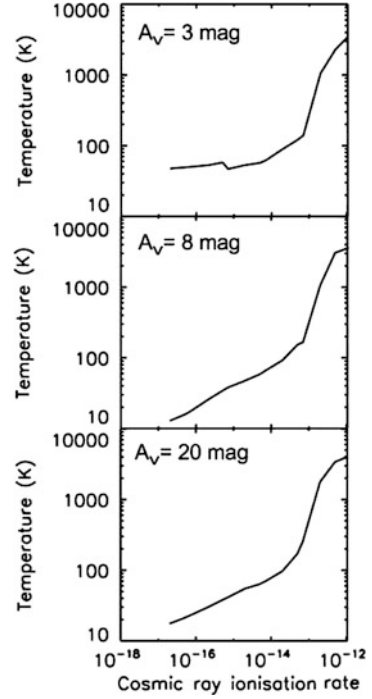
Can we determine useful molecular tracers of CRDRs? Bayet et al. [7] showed that it is necessary to make a complete and self-consistent thermal/chemical model of dense gas subjected to very high fluxes of cosmic rays in order to do so. They compute the variation of the chemistry as the ionization rate is increased for a large network of 131 species connected in 1,700 reactions in a self-consistent thermal/chemical and time-dependent one-dimensional model. The chemistry is computed using the UCL_PDR code [9] and ζ is varied from Milky Way values up to about one million times larger.

The UCL_PDR code is a time dependent photon dominated regions (PDR) model which self-consistently computes the thermal balance by taking into consideration all the relevant cooling and heating mechanisms [9]. Of particular importance for CRDRs is the inclusion of minor coolants such as the CO isotopologues, CS, H_2O and OH [7].

Figure 2 (reproducing Fig. 1 from Bayet et al. [7]) shows the gas temperature as a function of cosmic ray ionization rate for three different A_V : regardless of the visual extinction the temperature of course rises as ζ is increased. More interestingly, we find that the temperature at 20 mag is in fact higher than at 8 mag, due to the fact that lines of two of the main coolants, atomic carbon and carbon monoxide become optically thick and so the gas is not efficiently cooled. The most important implication is that, while at standard values of ζ the chemistry reaches equilibrium once photons stop dominating (i.e. at large enough visual extinctions), at very high cosmic ray ionization rates equilibrium may never be reached.

The chemistry of course gets affected by these high temperatures: Figs. 3 and 4 show the fractional abundances of several atomic and molecular species as a function of ζ for $A_V = 3$ and 20 mag. In general we find that a fairly rich chemistry can be maintained up to a critical value of ζ of 10^{-12} s^{-1} . The driver of the decline

Fig. 2 Taken from Bayet et al. ([7], Fig. 1): gas temperature in K as a function of ζ for three different visual extinctions



in molecular abundances is H_2 which starts declining at $\zeta \sim 10^{-14} \text{ s}^{-1}$. The resultant atomic hydrogen is very destructive. This together with the fact that the suppression of molecular hydrogen coincides with an abrupt increase in gas temperature assures fast dissociation for all molecules. Nevertheless we see that different species decline at different paces and times. While the chemistries at $A_V = 3$ and 20 mag are fairly similar, we note that at large depths higher molecular abundances are reached; in particular CS seems to be higher by a factor of 10^4 at 20 mag compared to its abundance at 3 mag.

While sulfur bearing species are confirmed as good sensitive tracers of ζ , regardless of visual extinctions ions *increase* with ζ . Interestingly HCO^+ , often used as a tracer of high cosmic ray ionizations regions, is not useful above $\zeta = 10^{-13} \text{ s}^{-1}$.

2.2 What Do Observations Tell Us?

The Bayet et al. [7] work, as well as others such as that presented in Meijerink et al. [24], give us some interesting and general conclusions on the temperatures achieved in these environments (e.g. much more elevated than in our own Milky Way up to values of 3,000 K or even higher) and on the chemistry, where it is found that even at ζ as high as 10^{-12} s^{-1} some, albeit few, molecular tracers exist (e.g. OH and OH^+) as well as, of course, atomic ones (C and C^+). However comparisons

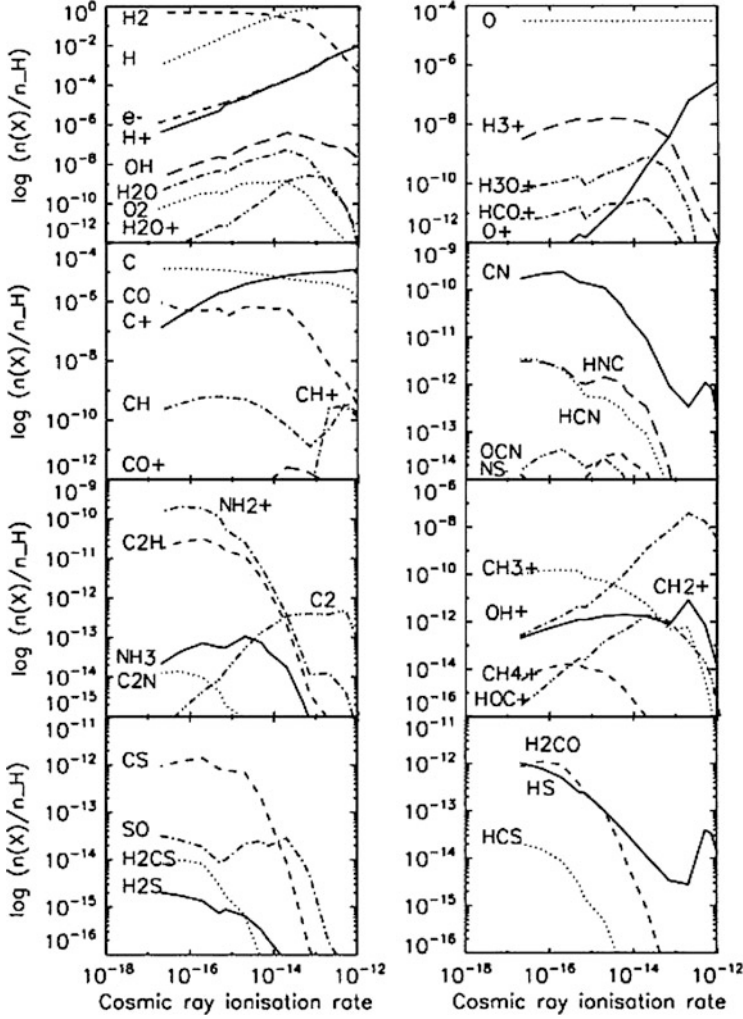


Fig. 3 Taken from Bayet et al. ([7], Fig. 2): fractional abundances of selected species as a function of ζ for a low metallicity environment (1/10 of solar) for $A_V = 3$ mag

with observations are needed in order to validate the relevance of these theoretical predictions for extragalactic studies.

It is convenient to compare theoretical predictions of chemistry in CRDRs with observations of starburst galaxies, since they have high cosmic ray energy density and possibly higher heating rates and higher ionization fractions. The best example is M82, an irregular starburst galaxy which is the most studied of all nearby galaxies. The high cosmic ray ionization rate has been postulated by e.g. the high C/C+ and C/CO ratios (e.g. [29]). Originating in the nucleus, the starburst activity within M82 is currently seen to be propagating into the molecular rings, disrupting the

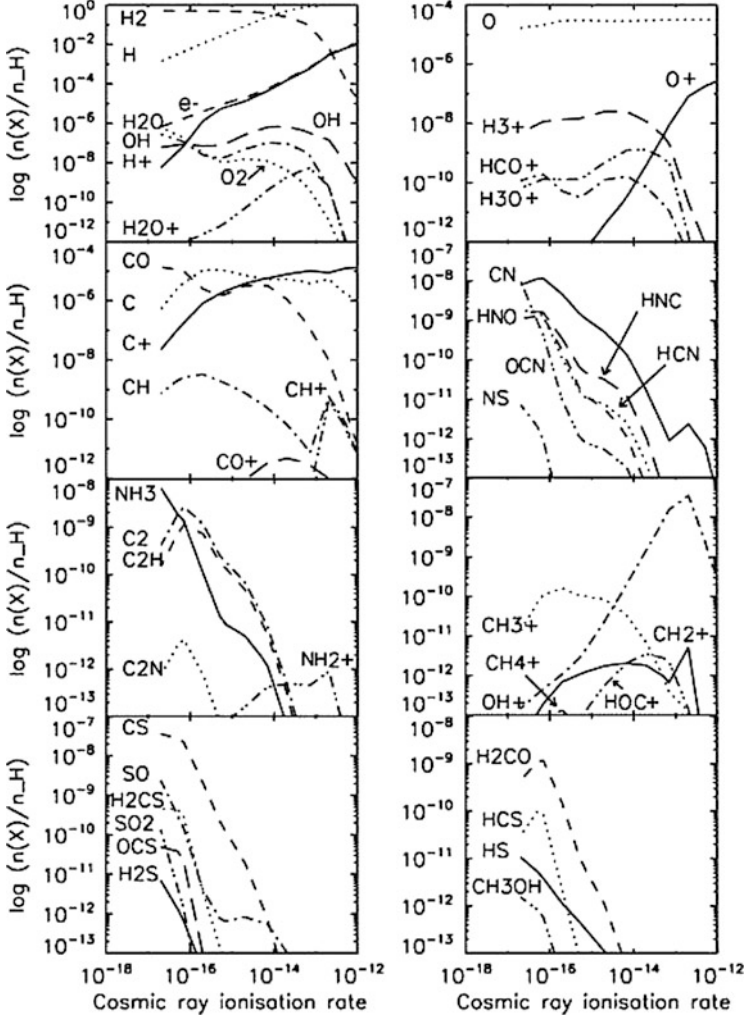


Fig. 4 Taken from Bayet et al. ([7], Fig. 4): fractional abundances of selected species as a function of ζ for a low metallicity environment (1/10 of solar) for $A_V = 20$ mag

surrounding ISM and causing the interstellar clouds to fragment. van der Tak et al. [31] detected the ion H_3O^+ in M82 and found a fractional abundance of $2\text{--}10 \times 10^{-9}$ which they could only match with a high ζ PDR, i.e. an evolved starburst. In fact, the Bayet et al. [7] models indicate that one can obtain high abundance of this ion at low (i.e. in a PDR) as well as high (i.e. dense star forming gas) extinction as long as $\zeta \sim 10^{-13} \text{ s}^{-1}$ and the metallicity is solar. At high extinction, which could represent the nuclear part of the galaxy, the abundance of H_3O^+ is higher, providing possibly a better match for the observations.

Ultra Luminous Infrared Galaxies (ULIRG) are also interesting objects where molecular ions are abundant: a high resolution SPIRE FTS spectrum of MrK 231 reveals the presence of ions such as OH^+ , CH^+ and H_2O^+ [32]. While abundances are not derived, van der Werf et al. [32] explained the high abundances of these ions by invoking X-rays and describing the emission as coming from X-ray dominated regions (XDRs); however Bayet et al. [7] shows that the type of model that is also able to produce high fractional abundances ($\geq 10^{-10}$) of these three ions is one representing an environment with low metallicity (0.1 solar), high cosmic ray ionization rates ($\geq 10^{-16} \text{ s}^{-1}$) and low visual extinction. Hence, as Papadopoulos [26] also points out, determining the origin of molecular emission from ULIRGs such as Mrk 231 is not trivial when both sources of energy (CR and X-rays) are present.

2.2.1 The Perseus Cluster

One of the most interesting clusters of galaxies where cosmic ray ionization rates may be much higher than in our own Galaxy is NGC1275, the Perseus cluster. In particular, this cluster contains filaments about 100 pc thick that are thought to originate from interactions between hot intercluster medium and relativistic plasma associated with AGN (e.g. [21]). Ferland et al. [14, 15] modelled optical and IR emission arising from gas heated by dissipation and cosmic rays and found that the best models required heating rates several orders of magnitudes higher than in our own galaxy. Bayet et al. [6] explored the chemistry of molecular regions subject to heating rates per volume and cosmic ray ionisation rates per particle in ranges suitable for the NGC 1275 filaments. They identify detectable molecular species that may provide a diagnostic of the dissipation heating as well as the cosmic ray ionization rate. Figure 5 (Fig. 3 from Bayet et al. [6]) compares the chemistry, density and temperature for a low and a high cosmic ray ionization regime, both with an additional heating source. They find that, unfortunately, it is not easy to distinguish between additional heating sources and enhanced cosmic ray ionization rates by looking at the chemistry. However, the molecular species HCO^+ , C_2H and CN are certainly good tracers of heating in these filaments and their abundance ratios may provide a way of disentangling the effects of a high cosmic ray ionization rate from that of an additional heating source.

Therefore, the same authors followed up these predictions with an observational campaign of the Perseus central region and filaments [8]. They detected for the first time emission lines of $\text{CN}(2-1)$, $\text{HCO}^+(3-2)$ and $\text{C}_2\text{H}(3-2)$ in two positions: directly at the central galaxy, NGC1275, and also at a position about $2''$ to the east where associated filamentary structure has been shown to have strong CO emission. In the central region, there is a clear detection in CN and HCO^+ and a weak detection of the C_2H transition; in the filamentary structure weak detections of CN and HCO^+ were found. Crude estimates of the column densities and fractional abundances were compared with the Bayet et al. [6] models and it was found that the models in which heating is caused mainly by cosmic rays can account for the molecular observations. However, the cosmic ray heating rate needs to be at least two orders of magnitude larger than that in the Milky Way.

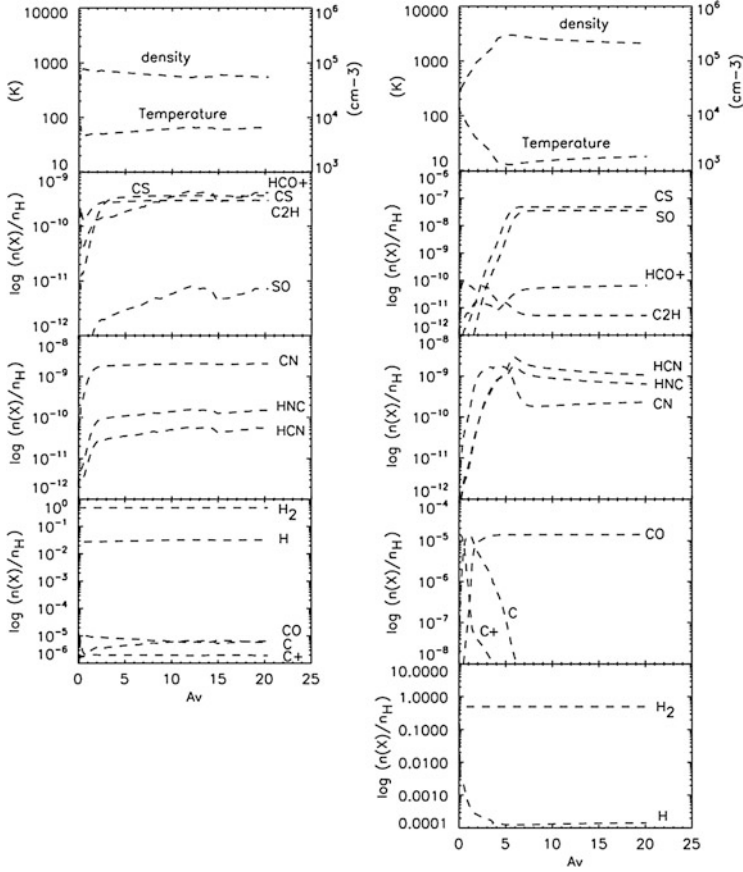


Fig. 5 Taken from Bayet et al. ([6], Fig. 3): temperature, density and selected fractional abundances as a function of visual extinctions for $\zeta = \times 10^{-15} \text{ s}^{-1}$ (Left) and $\zeta = \times 10^{-17} \text{ s}^{-1}$ (Right); both models also have an additional source of heating included

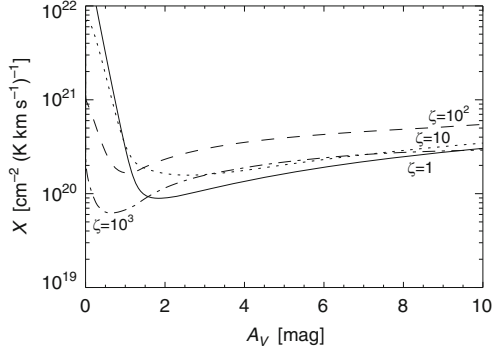
3 Cosmic Rays and the X Factor

Another indirect effect of high cosmic ray ionization rates is on the CO-to-H₂ conversion factor, often used to determine the mass of galaxies since, unlike molecular hydrogen, CO is readily observable. This factor is usually expressed by the equation:

$$X = \frac{N(\text{H}_2)}{\int T_A(\text{CO}) dv} \quad (1)$$

in units of $[\text{cm}^{-2}(\text{K km s}^{-1})^{-1}]$ and where $N(\text{H}_2)$ is the column density of H₂ and $T_A(\text{CO})$ is the antenna temperature of the CO(1-0) line (see e.g. reviews by Maloney [22], Combes [12], and Young [34]). Bell et al. [9] explored the sensitivity

Fig. 6 The X factor as a function of A_V for various ζ (Adapted from Fig. 5 of Bell et al. [9])



of this factor for a range of conditions including variations in the cosmic ray ionization rate. Figure 6 shows the influence of varying ζ on the X factor. The characteristic depth profile of the X factor has three main features: near the outer edge of the cloud, where the H/H_2 transition occurs and H_2 is present without CO , X is large. As we move towards higher depths, all hydrogen is in molecular form, CO self-shielding becomes sufficiently strong to prevent photodissociation, and this allows its abundance and emission strength to rise sharply. This causes X to drop, reaching a minimum value in the region where CO emission is strongest. As the CO line becomes optically thick with increasing depth, local emission gradually declines and X begins to rise slowly again. It is indeed this minimum of the depth profile that determines X because it corresponds to the peak emission of the CO line. From Fig. 6, one sees that as the ionization rate increases from the standard value, CO is initially destroyed more effectively (through reactions with He^+) and its abundance drops, causing an upward shift in the X profile. However, the corresponding increase in the cosmic ray heating rate causes a rise in gas temperature, becoming the dominant heating mechanism. This promotes CO formation and emission, and counters, in part, the increased destruction rate. The X profile minima become lower and nearer the cloud surface. Thus, a slight rise in ionization rate shifts the X profile minimum upwards, whilst a further increase in ionization rate leads to the X minimum dropping and moving towards the cloud surface. So, in summary, X increases as ζ increases up to 100 times the standard value, but then decreases as ζ approaches 10^{-14} s^{-1} ; the profile is raised due to the dissociation of CO ; the subsequent lower and sharper minimum is due to the increased OH formation and dissociation of H_2 .

3.1 The X Factor in Starburst Galaxies

The X factor as defined in Eq. 1 for $\text{CO}(1-0)$ may also be defined for other transitions in CO as well as for transitions in atomic and molecular species other than

Table 2 Values for the CO-to-H₂ and C-to-H₂ conversion factors for starburst galaxies. Values of X_{CO} and X_{CI} are given in units of $10^{20} \text{ cm}^{-2} (\text{K km s}^{-1})^{-1}$

Galaxy	$J = 1 \rightarrow 0$	$J = 2 \rightarrow 1$	$J = 3 \rightarrow 2$	$J = 4 \rightarrow 3$	$J = 6 \rightarrow 5$	$J = 9 \rightarrow 8$	[CI] 609 μm
NGC6946	0.2	0.1	0.1	0.2	0.6	2.3	0.4
M82	1.5	1.7	2.9	9.5	79.4	203.7	1.3

CO [25,28]. Bell et al. [10] computed suitable CO-to-H₂ (for several transitions) and C-to-H₂ conversion factors for several galaxy types, including regular and irregular starbursts. They chose NGC6946 as a prototype regular starburst, while M82 as a prototype irregular starburst, as examples of their applications. In order to derive appropriate physical parameters for these galaxies, they compared emission line intensity ratios predicted by their PDR models to those observed. The best-fitting models were determined by performing a χ^2 fit for several atomic and molecular ratios:

1. OI(63) μm /CII
2. OI(145) μm /OI(63) μm
3. CII/CI(609) μm
4. CII μm /CO(3-2)
5. CI(609) μm /CO(3-2)
6. CO(3-2)/CO(1-0)

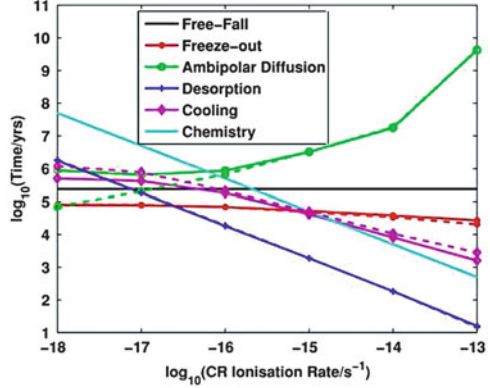
Table 2 summarizes their results for NGC6946 and M82.

Interestingly Bell et al. [10] found that the best χ^2 fit for both types of starburst galaxies was reached for standard cosmic ray ionization rates, apparently in contrast with the results from Bayet et al. [7]. However, Bell et al. [10] point out that for M82 the models with cosmic ray ionization rates of 10 and 100 times higher produce χ^2 values which are only 3 and 2 higher than that for the best fit model, respectively. Moreover the line ratios considered in Bell et al. [10] are not necessarily sensitive to the conditions in CRDR environments: for example the [CII] and [OI] lines trace only the PDR surfaces, not the dark regions where cosmic rays would be most important.

4 Cosmic Rays and Their Influence on the Low Mass Star Formation Rate

Estimates of the evolution of the space density of the massive star-formation rate are routinely made [17, 19, 20], and, although very uncertain, at least they provide some constraints for the high end of the Initial Mass Function (IMF). On the other hand, there is very little information on the formation of extragalactic low mass stars, which may influence galaxy formation and evolution by shaping the IMF and its slope.

Fig. 7 Taken from Banerji et al. ([3], Fig. 1): Timescales for different processes as a function of ζ



Low-mass star formation (at least in the Milky Way) is controlled by several critical timescales associated with processes such as gravitational collapse and thermal and magnetic support, cooling, ionization and hence chemistry, which itself is moderated by cosmic ray and photon fluxes, and metallicity. While in our own Galaxy these timescales are such that they favour formation of low mass stars, the physical properties in external galaxies may depart significantly from the Milky Way values. Banerji et al. [3] computed how these relevant timescales may vary when physical conditions are modified from Milky Way values and used the results to determine the regions of parameter space in which low-mass star formation is unlikely to occur. Banerji et al. [3] computed these timescales for a large range of physical conditions ($n_H = 10^2 - 10^6 \text{ cm}^{-3}$; metallicity = $(10^4 - 3) \times \text{solar}$; ζ : $10^{-18} - 10^{-13} \text{ s}^{-1}$; FUV: $(1 - 10^4) \times \text{FUV}_{\text{MilkyWay}}$) in order to represent a wide range of galaxy types. We show in Fig. 7 (taken from [3]) how the different timescales vary with cosmic ray ionization rate.

As one can see from Fig. 7, as ζ increases, the cooling time falls and when ζ has increased to 10^{-16} s^{-1} it drops below the free fall time. As a consequence more cores should be able to collapse because the chemistry is also quick, again due to the high cosmic ray ionization rate. The freeze out time is longer than desorption time, hence molecules remain in the gas for longer periods and cool the gas, again in favour of high rates of star formation. However ambipolar diffusion, the process by which, due to low ionization, the field lines decouple from the neutral matter allowing therefore the material to drift in response to the gravitational potential, will be very slow as ions do indeed increase; this implies that star formation may not be viable in clouds that are magnetically subcritical under these conditions and, hence, depending on the magnetic field, collapse may be halted, possibly resulting in a high-mass-biased stellar IMF.

Chemistry may produce tracers of top-heavy stellar IMF. This is explored in Banerji et al. [4]; the authors find that while the rotational distribution of CO should be similar between galaxies with top-heavy IMFs and those with unbiased IMFs, the high-J to peak CO ratio differs according to their metallicity and can therefore

be used to roughly infer the metallicity of a galaxy provided we know whether it is active or quiescent. The metallicity strongly influences the shape of the IMF. They also find that CS may be a good tracer of metallicity while HCN, HNC, and CN are found to be relatively insensitive to the IMF shape at the large visual magnitudes typically associated with extragalactic sources.

5 Conclusions

Cosmic rays initiate and very quickly affect the chemistry of the interstellar medium (ISM). It is therefore crucial to accurately determine the cosmic ray ionization rate, ζ , in the ISM. Clearly, the rate may vary among galaxy types. In our own Galaxy it is believed to be $\sim 10^{-17} \text{ s}^{-1}$ although studies of the diffuse medium may indicate a somewhat higher value. In active galaxies, such as starburst or AGNs, ζ is certainly larger than 10^{-17} s^{-1} . High ζ will increase the average kinetic temperature of the gas (to possibly over 3,000 K for $\zeta = 10^{-12} \text{ s}^{-1}$). We find that chemistry can indeed still trace the cosmic ray ionization rate, up to $\zeta = 10^{-12} \text{ s}^{-1}$. However interpreting atomic and molecular observations of starburst galaxies in order to trace the cosmic ray ionization rate is not trivial, as ζ is likely to spatially vary. Another important consequence of variations in the cosmic ray ionization rates is its non linear influence on the X factor and one must take care when estimating molecular masses from CO if ζ is not known. Finally, because the cosmic ray ionization rate influences the star formation rate, there may be important consequences for the Initial Mass Function at high redshift.

References

1. Acciari, V. A., Aliu, E., Arlen, T., et al. 2009, *Nature*, 62, 770
2. Acero, F., Aharonian, F., Akhperjanian, A. G., et al. 2009, *Science*, 326, 1080
3. Banerji, M., Viti, S., Williams, D. A., Rawlings, J. M. C., 2009a, *ApJ*, 692, 283
4. Banerji, M., Viti, S., Williams, D. A., 2009b, *ApJ*, 703, 2249
5. Bayet, E., Viti, S., Williams, D. A., Rawlings, J. M. C., Bell, T. A., 2009, *ApJ*, 696, 1466
6. Bayet, E., Hartquist, T. W., Viti, S., Williams, D. A., Bell, T. A., 2010, *A&A*, 521, A16
7. Bayet, E., Williams, D. A., Hartquist, T. W., Viti, S., 2011a, *MNRAS*, 414, 1583
8. Bayet, E., Viti, S., Hartquist, T. W., Williams, D. A., 2011b, *MNRAS*, 417, 627
9. Bell, T. A., Roueff, E., Viti, S., Williams, D. A., 2006, *MNRAS*, 371, 1865
10. Bell, T. A., Viti, S., Williams, D. A., 2007, *MNRAS*, 378, 983
11. Black, J. H., Dalgarno, A., 1977, *ApJS*, 34, 405
12. Combes, F., 1991, *ARA&A*, 29, 195
13. Draine, B. T., 2011, “Physics of the Interstellar and Intergalactic Medium”, Princeton Series in Astrophysics.
14. Ferland, G. J., Fabian, A. C., Hatch, N. A., Johnstone, R. M., Porter, R. L., van Hoof, P. A. M., Williams, R. J. R., 2008, *MNRAS*, 386, 72
15. Ferland, G. J., Fabian, A. C., Hatch, N. A., Johnstone, R. M., Porter, R. L., van Hoof, P. A. M., Williams, R. J. R., 2009, *MNRAS*, 392, 1475

16. Hartquist, T. W., Black, J. H., Dalgarno, A., 1978, MNRAS, 185, 643
17. Hopkins, A. M., & Beacom, J. F., 2006, ApJ, 651, 142
18. Indriolo, N., Geballe, T. R., Takeshi, O., McCall, B. J., 2007, ApJ, 671, 1736
19. Lilly, S. J., Le Fevre, O., Hammer, F., Crampton, D., 1996, ApJ, 460, 1
20. Madau, P., Ferguson, H. C., Dickinson, M. E., Giavalisco, M., Steidel, C. C., Fruchter, A., 1996, MNRAS, 283, 1388
21. McNamara, B. R., O’Connell, R. W., Sarazin, C. L., 1996, AJ, 112, 91
22. Maloney, P., 1990, ApJ, 348, 9
23. Meijerink, R., Spaans, M., Israel, F. P., 2006, ApJ, 650, 103
24. Meijerink, R., Spaans, M., Loenen, A. F., van der Werf, P. P., 2011, A&A, 525, 119
25. Papadopoulos, P. P., Thi, W.-F., Viti, S., 2004, MNRAS, 351, 147
26. Papadopoulos, P. P., 2010, ApJ, 720, 226
27. Papadopoulos, P. P., Thi, W.-F., Miniati, F., Viti, S., 2011, MNRAS, 414, 1705
28. Sakamoto K., Okumura S. K., Ishizuki S., Scoville N. Z., 1999, ApJS, 124, 403
29. Schilke, P., Carlstrom, J. E., Keene, J., Phillips, T. G., 1993, apJ, 417, 67
30. Suchkov, A., Allen, R. J., Heckman, T. M., 1993, ApJ, 413, 542
31. van der Tak, F. F. S., Aalto, S., Meijerink, R., 2008, A&A, 477, 5
32. van der Werf, P. P., Isaak, K. G., Meijerink, R., et al., 2010, A&A, 518, 42
33. Webber, W. R., Yushak, S. M., 1983, ApJ, 275, 391
34. Young, J. S., Scoville, N. Z., 1991, ARAA, 29, 581

Cosmic Rays in Star-Forming Environments
Proceedings of the Second Session of the Sant Cugat
Forum on Astrophysics
Torres, D.F.; Reimer, O. (Eds.)
2013, XVI, 446 p., Hardcover
ISBN: 978-3-642-35409-0